Electronic Journal of Biotechnology 57 (2022) 44–51

Contents lists available at ScienceDirect

Electronic Journal of Biotechnology

journal homepage:

Research Article

Self-contained and integral microbial fuel cells as portable and sustainable energy sources for low-power field devices

Naroa Uria-Molto [a,*], Ruben D. Costa [a], Cybeles Nunziata [a], Sara Santiago [b,c], Gonzalo Guirado [c], Xavier Muñoz-Berbel [b], Lukasz Kowalski [a]

[a] Arkyne Technologies SL (Bioo) ES-B90229261, Carrer de La Tecnologia, 17, 08840, Viladecans, Barcelona, Spain
[b] Instituto de Microelectrónica de Barcelona, IMB-CNM (Consejo Superior de Investigaciones Científicas), 08193, Esfera UAB, 08193, Bellaterra, Barcelona, Spain
[c] Departament de Química, Universitat Autònoma de Barcelona, Bellaterra, Barcelona 08193, Spain

GRAPHICAL ABSTRACT

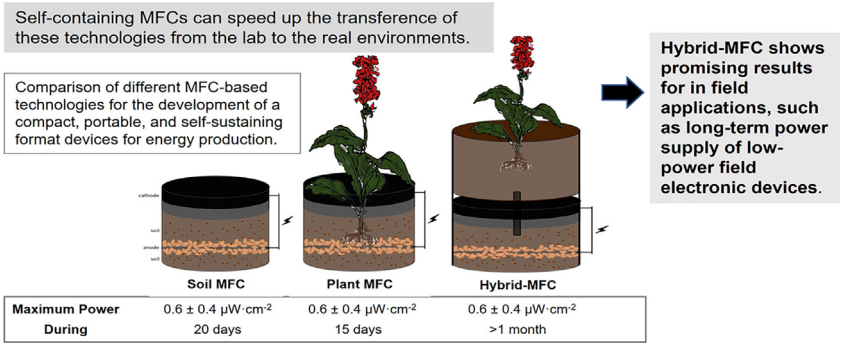

ARTICLE INFO

Article history:
Received 16 December 2021
Accepted 11 April 2022
Available online 19 April 2022

Keywords:
Hybrid-microbial fuel cell
Internal resistance
Plant microbial fuel cell
Portable devices
Power harvesting
Soil-microbial fuel cell

ABSTRACT

Background: With a smaller environmental footprint and longer operation times, Microbial Fuel Cells (MFCs) are now preferred over other renewable technologies for powering small electronic devices in the field. Although with excellent performance in the laboratory, most of MFCs fail for not considering the real field conditions. The purpose of this study is the development of a compact, portable, and self-sustaining format of energy production based on MFC technologies. For this, three MFC configurations, soil MFC, plant MFC and a hybrid-MFC, where a plant and a soil MFC are combined, are assembled in portable power devices and compared.
Results: Plant MFCs provided lower performances (maximum power of 0.6 ± 0.4 $\mu W \cdot cm^{-2}$) resulting from a fast and sharp decrease in the anode potential by the flowing of oxygen from the aerenchyma of the plant roots. The performance of soil MFCs was much better (maximum power of 2.0 ± 0.02 $\mu W \cdot cm^{-2}$), but not sustained over time (20 days) by the depletion of organic matter. The combination of a soil MFC and a plant in separate compartments of a single container results in a hybrid-MFC with a good performance (maximum power of 2.7 $\mu W \cdot cm^{-2}$) which sustained over time for more than 1 month.
Conclusions: Therefore, the hybrid self-containing MFCs appears as an ideal alternative for the long-term power supply of low-power field electronic devices, from meteorological sensors or LED lights.

Peer review under responsibility of Pontificia Universidad Católica de Valparaíso
* Corresponding author.
E-mail address: naroa@bioo.tech (N. Uria-Molto).

https://doi.org/10.1016/j.ejbt.2022.04.004

How to cite: Uria-Molto N, Costa RD, Nunziata C, et al. Self-contained and integral microbial fuel cells as portable and sustainable energy sources for low-power field devices. Electron J Biotechnol 2022;57. https://doi.org/10.1016/j.ejbt.2022.04.004

1. Introduction

Environmental pollution, global warming, and energy shortage have led the search for sustainable and environmentally friendly energy production methods and technologies. Photovoltaic solar panels have been the flagship technology used to substitute conventional chemical batteries since enabling delocalized power supply, with high power yields and with minimal residue production. However, other renewable energy sources are now explored to minimize the cost, environmental footprint, visual impact, and intermittence in power supply of solar panels. One of the preferred alternatives is Microbial Fuel Cells (MFCs) [1], where microorganisms, named electrogenic, convert the chemical energy stored in biodegradable substances into electrical current [2,3,4]. In general, this technology has a widespread implementation potential for the ubiquity of electrogenic bacteria, nearly present in every kind of soil, and the capacity to operate satisfactorily in mild environmental conditions (between 20 and 40°C, at pH 7). The use of microorganisms as biocatalyst has additional advantages, such as a reduction in cost and potential toxicity of the system, and self-healing capacity by the living and proliferating nature of bacteria. The MFC can thus produce energy continuously (24 h/d), for long time periods and with minimal maintenance requirements.

Two main technologies derived from MFCs are preferably considered for in field applications since obtaining the energy directly from nature. First, sediment or soil-MFCs (sMFC), where an anode and a cathode are placed in the sediment and water, respectively, and the current is generated by oxidizing on the anode present in the sediment, and the oxygen reduction action occurs on the cathode in water [4,5]. On the other hand, plant-MFCs (pMFC) integrate plants and microorganisms to convert chemical energy into electrical energy [6]. Although with enormous similarities, they differ in the fuel supply. While in sMFC the organic matter for microbial energy production comes directly from the soil and depends on its initial composition, the nutrient supply in pMFC is continuous, resulting from plant photosynthesis [7]. The plant extends, therefore, the lifetime of bacteria and the fuel cell [8], but it also links power efficiency with any factor affecting plant metabolism, e.g. the number of daylight hours, the efficiency of the photosynthetic process or the allocation of organic matter from plant to soil [9,10]. Additionally, the production of oxygen in the plant-roots and its transport to the anode reduces the efficiency of the process, decreasing the number of electrons available and the anode potential [9]. Thus, there is no ideal MFC technology, but each presents advantages and disadvantage in power supply.

Due to their capacity to provide low (hundreds of μW) but almost constant power supply over time [8,11], both sMFCs and pMFCs have been already implemented as energy sources in self-powered electronic devices for environmental monitoring [12], control of plant maturity [13], bioremediation and heavy metals recovery [14,15]. Although performing well in the laboratory, their problems start when implemented in the field, under real environmental conditions, where plants and soil compositions widely differ from those used in the laboratory [16]. Thus, to the best of our knowledge, only one recent work has presented a portable sMFC for electricity generation [17].

This article presents self-containing fuel cell architectures for optimal transference of MFCs from the laboratory to the field. This integral solution consists of a pot-like cell design where, soil and plant previously selected in the laboratory, are introduced, and maintained under optimal conditions, with the same soil used in the laboratory and in a close device preventing possible damage to MFC components. When implemented in the field, the conditions inside the cell exactly replicate those of the laboratory, ensuring optimal performance at any environment condition. Three configurations are developed and implemented in portable power devices and compared in terms of power supply and long-term stability. The objective of the work was to find out the best green and ready to use solution for energy production in a compact, portable, self-sustaining format.

2. Material and methods

2.1. Experimental set-up

A total of 3 replicates for pMFC and sMFC were constructed using the same setup and filled with soil (Organic potting soil, Burés, S.A). In the case of pMFCs, a previously grown *Canna indica* in vegetative phase were planted.

MFC reactors consisted of a cylinder-shaped polyvinyl chloride (PVC) container of 11 cm diameter and 10 cm height with the upper face open. The anode and cathode electrodes were made of graphite felt (AvCarb® G300) of 3 mm thick and 95 cm^2. In both cases (sMFC and pMFC), 1 cm of soil was placed at the bottom of the container just below the anode, which had a circular shape with 11 cm diameter. Then, nitrate-less ammonium-bicarbonate-rich ½ modified Hoagland solution (N-AB + H solution) (Fig. S1) [18] was added until flooded. *Canna indica* root balls were placed

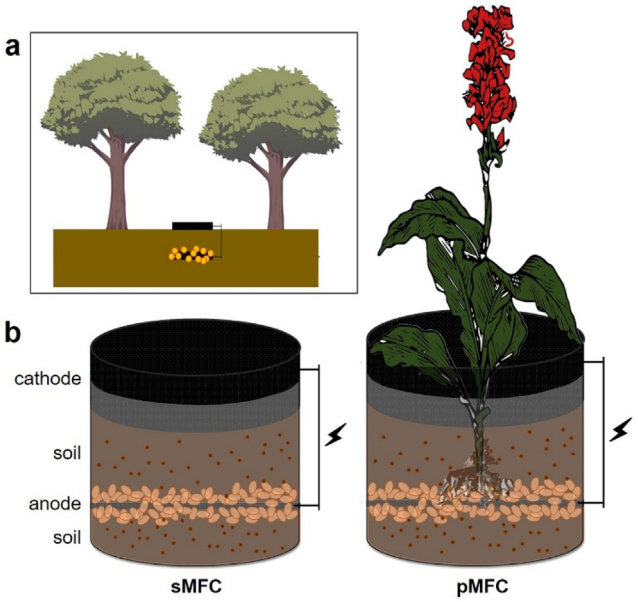

Fig. 1. (a) Schematic image of a typical soil-MFC in field with an anode buried in the soil and a cathode in the surface. (b) Schematic representation of the pot-like MFCs, soil-MFC (sMFC) using a universal horticultural soil and a plant-MFC (pMFC) using *Canna indica*.

on top of the pMFC anodes and soil was added until reaching a height of 5 cm.

In the case of sMFCs, the containers were filled at the same height only with soil. The cathode electrodes were cut into a 33 cm × 6 cm rectangle shape (198 cm^2) and placed on top of the flooded soil in contact with the container internal wall. Then, soil was added until reaching the top burying it partially. Approximately 3 cm, half of the cathode rectangular electrodes, remained buried and 3 cm out of the container (Fig. 1b).

sMFC and pMFC reactors worked inside a climatic chamber with controlled temperature, humidity, and light conditions. Inside the climatic chamber, the temperature was maintained to 26°C, while humidity was controlled through a humidifier device with values between 40 and 50%. Additionally, the climatic chamber included LED lights to simulate sunlight connected to an Arduino device that automatically turns on and off the lights following a preprogrammed photoperiod, emulating day/light cycles in the real environment. The MFCs were fed daily with N-AB + H solution via a pump to maintain the system flooded.

2.2. MFC operation

Following inoculation, the MFCs were operated for a period of 31 d under a constant load of 1 kΩ only interrupted during Open Circuit Potential (OCP) measurement and Linear Sweep Voltammetry (LSV) measurements, which executed once a week.

When working in close circuit with 1kΩ load, the permanent monitoring of the voltage drop on the resistor was registered by in-house voltage data logger built on top of Arduino platform (Fig. S1).

To perform voltage measurements the commercially available Arduino Nano system was used. Arduino Nano microprocessor board is equipped with10-bit Analog to Digital Converter (ADC) which can be further set with either 5 V or 3.3 V range or INTERNAL reference voltage source of 1.1 V. Setting this last one 1.1 voltage feature and taking in mind that 10-bit is an equivalent of 1024 (2^10) states we achieve the resolution of Less Significant Bit (LSB) of 1.074 mV that can be directly calculated from equation 1.1 V/1024. The measurements were taken with maximum frequency to provide averaged results for every 1 minute of experiment. A resolution of 1 μV for voltage measurements was achieved.

The current (I) generated by each microbial cell was found from the Ohm's law expression:

$$I = \frac{U}{R}$$

where U is the potential obtained at a given resistance, and R is the applied resistance, and calculated as follows:

$$I = \frac{U_{ADC}}{1k\Omega}$$

Similarly, the power (P) obtained by the reactors was obtained from the expression:

$$P = U \cdot I$$

which is:

$$P = U_{ADC} \cdot I = \frac{{U_{ADC}}^2}{1k\Omega}$$

Current and power values were normalized by the anode area.

Finally, the energy (E) generated by each reactor during the whole experiment was calculated as:

$$E = P \cdot t_s$$

where t_s is the sampling time, in our case 60 s.

2.3. Electrochemical measurements

Electrochemical measurements were performed using a Portable Multi Potentiostat μSTAT 4000P (Metrohm DropSens, Spain) and DropView 8400 software (DropSens, Spain).

For MFC characterization, I-V curves were built and the OCP, current output (Imax) and power output (Pmax) parameters were determined weekly, enough time to observe differences in the parameters studied due to the growth of the cells.

I-V curves were performed by Linear sweep voltammetry method (LSV), an electrochemistry technique that allows cycling over the potential range from the upper potential limit to the lower potential limit. Potential range started 50 mV above the OCP down to 0 V, and the current was recorded with a step resolution of 1 mV at a scan rate of 1 $mV \cdot s^{-1}$. After this, power was calculated following the equation:

$$Power = Voltage\ difference \cdot Current$$

and power curves were constructed by representing this value in front of the current.

To determine the OCP value, MFCs were kept without load for about 1 h to ensure cells potential stabilization. Then, Zero Current Potentiometry (ZCP) mode was applied for 10 min with 0.5 s voltage sampling time. The last measured value was considered as the OCP.

Anode potential of each MFC was measured in open circuit condition previously to electrochemical recording. The I-V curve was obtained after placing an Ag/AgCl reference electrode (Methrom, Switzerland) inside the MFCs and close to the anode. The corresponding voltage (OCP_{anode}) between reference electrode and anode was measured using multimeter FORTEX UT58C. Cathode potential was calculated as the sum between the OCP and anode potential (OCP_{anode}) obtained for each MFC.

At the end of experimental phase, the electrogenic community forming the anode biofilm was analysed by Cyclic Voltammetry (CV). For this, the anodes of the different MFCs were removed from each reactor and washed several times in phosphate-buffered saline (PBS, Sigma Aldrich) to remove soil remains and other substances from the electrode. Anode electrode fragments of 1 cm^2 were used as the working electrode submerged in an electrochemical cell containing 100 mL of PBS flushed with nitrogen gas to eliminate oxygen. An Ag/AgCl electrode (Methrom, Switzerland) and a graphite felt electrode with an area of 20 cm^2 were used as reference and auxiliary electrode, respectively. CV experiments were run between −0.6 V and +0.6 V (vs. Ag/AgCl) at a scan rate of 5 $mV \cdot s^{-1}$.

2.4. Bacteria concentration and pH measurements

Bacteria concentration present in the soil used in the MFC reactors before and after MFC operation was determined by serial dilutions and plate counting in aerobic and anaerobic conditions. For this, 1 g of soil was added to 9 mL of Ringer (0.9% NaCl, Sigma Aldrich) and, after a gentle agitation, serial dilutions were prepared with Ringer solution and plated in Tripticase Soy Agar (TSA, Sigma Aldrich). After 48 h incubation at 30 °C, bacteria concentration was calculated by the following expression:

$$cfu \cdot mL^{-1} = \frac{colonies}{plated\ \ volume(mL) \cdot plated\ dilution}$$

For anaerobic bacteria counts, plates were growth inside an anaerobic jar (28029-1EA-F, Sigma-Aldrich; Merck KGaA, Darmstadt, Germany) with anaerobic atmosphere generation bags

(68061-10SACHETS-F, Sigma-Aldrich; Merck KGaA, Darmstadt, Germany) coupled with an indicator test (59886-1PAK-F, Millipore; Merck KGaA, Darmstadt, Germany).

pH measurements of the MFCs were performed at the beginning and the end of the experiment. Samples of about 5 mL of the water flooding the soil and plant roots were taken and measured with a Nahita Lab pHmeter model 903.

2.5. Statistical analysis

The significant difference in aerobic and anaerobic microbial biomass and maximum power obtained by sMFC and pMFC reactors was determined by ANOVA at the level of $p < 0.05$. All statistical tests were performed using R software (version R 4.0.2).

2.6. Design of self-contained hybrid architectures with combination of soil and plant MFCs

The first prototype of a hybrid device consisted of two polyvinyl chloride (PVC) compartments. A sMFC was placed in the lower part, while in the upper part a tank with the plant was located. Between the two compartments there was a space through which air could circulate. In addition, these containers were connected by a tube allowing the leachate originated by the irrigation water of the plant to circulate and penetrate the upper part of the MFC compartment.

The lower tank (sMFC) had a dimension of 30 cm × 30 cm and a depth of 10 cm with the upper face open. The anode and cathode electrodes with square shape of 30 cm side were made of graphite felt (AvCarb® G300) of 3 mm thick. One cm of soil was placed at the bottom of the container just below the electrode acting as the anode, while in the upper part, in contact with the air, the cathode was placed. Between the electrodes, the sMFC was filled with horticultural soil. In the upper part of the hybrid device, the tank that housed the plant had dimensions of 30 cm × 30 cm and 5 cm deep.

3. Results and discussion

3.1. Study of microbial biomass and pH variation in self-containing sMFC and pMFC

Since microbial energy production depends on the nature and quantity of the microorganisms in the fuel cell, the variation in microbial biomass over time was analysed in the two cases. Both MFCs were prepared in similar conditions, with the main difference of the presence of the plant in the case of pMFCs. At the beginning of the experiment, the two MFC reactors presented identical amounts of aerobic and anaerobic bacteria, $4.8{\cdot}10^4$ cfu·mL^{-1} for aerobic and $2.53{\cdot}10^3$ cfu·mL^{-1} for anaerobic. After 31 d of continuous operation, the biomass increased in both MFC, confirming that energy production in these configurations did not affect bacterial growth. Additionally, the fluctuations in biomass concentration between the two types of MFC system (sMFC and pMFC) were not significant ($p > 0.05$), being of $3.89{\cdot}10^6$ and $3.13{\cdot}10^5$ cfu·mL^{-1} for aerobic and anaerobic bacteria in pMFC reactors, and $3.40{\cdot}10^6$ cfu·mL^{-1} and $5.69{\cdot}10^5$ cfu·mL^{-1} for sMFCs. The result indicated that the plant in the pMFC reactors did not improve the microbial growth.

Considering pH, both cells presented a slightly basic pH at the beginning of the experiment, i.e. 7.75 ± 0.17 (pMFC) and 8.12 ± 0.00 (sMFC), although the pH in the rhizosphere of plants is generally slightly acidic (pH 5–6). Along the experiment, the pH slightly decreased in both MFCs, until reaching an almost neutral pH of 6.45 ± 0.08 (pMFC) and 6.80 ± 0.06 (sMFC) at the end of the experiment. This result was in agreement with previous works in pMFCs, where medium acidification was also observed due to current generation [9,19].

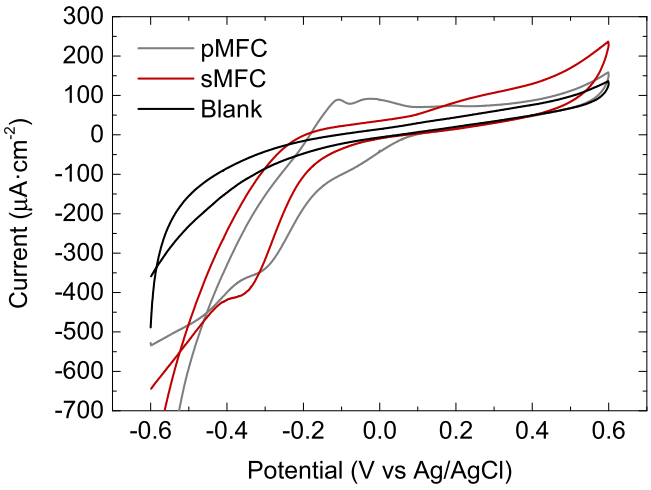

Fig. 2. Cyclic voltammetry at a scan rate of 5 mV·sec^{-1} and a scan range between −0.6 and 0.6 V of a 1 cm^2 fragment of sMFC and pMFC graphite felt anodes and a blank (a new graphite felt electrode) in phosphate buffer saline flushed with nitrogen.

3.2. Electrochemical analysis of the biofilms

In order to verify the electrochemical activity of the biofilm formed on the anode at the end of the experiment, cyclic voltammetry experiments (CV) analysis was conducted for sMFCs and pMFCs anodes. As shown in Fig. 2, both anodes presented additional oxidation–reduction peaks that confirmed the presence of bacterial biofilms with electron exchange capacity.

Although in MFC-based reactors the catalytic current was significantly higher than in the blank, i.e. a graphite felt electrode without biofilm, both anodes presented different redox peaks and species involved in electron exchange and energy production. The voltammogram of the pMFC biofilm indicated the existence of one reversible redox specie with potential values of −0.095 and −0.295 V (vs Ag/AgCl). On the other hand, sMFC showed a reduction peak at a potential of −0.351 V (Ag/AgCl) with no clear oxidation peaks (irreversible redox specie). The presence of the plant was thus favouring the proliferation and colonization of the anode by bacterial species present in the soil but not very comfortable with its initial conditions. This differential biofilm composition and redox species involved in the production of energy may influence the performance and stability of the MFCs, which analysed in the following section.

3.3. Self-contained MFCs' long term electrical performance and characterization

Three replicates of the sMFC and pMFCs were run in parallel under the same conditions for 5 weeks, and voltage was recorded with an external load of 1 kΩ. Current was produced in all reactors while plants in pMFCs increased in size and height indicating no MFC operation effect in plants growth.

After a start-up period of 3 d, pMFC reactors' voltage started to increase until reaching a maximum and stabilizing at d 6. After this, power was stable with an average of 0.5 ± 0.08 μW·cm^{-2} until d 15, when power started to decrease. Two power spikes observed at days 26 and 27 were produced by a problem with the energetic supply. The reconnexion of the devices carried out this effect that it was recovered quickly. Moreover, a day-night cycle independent of

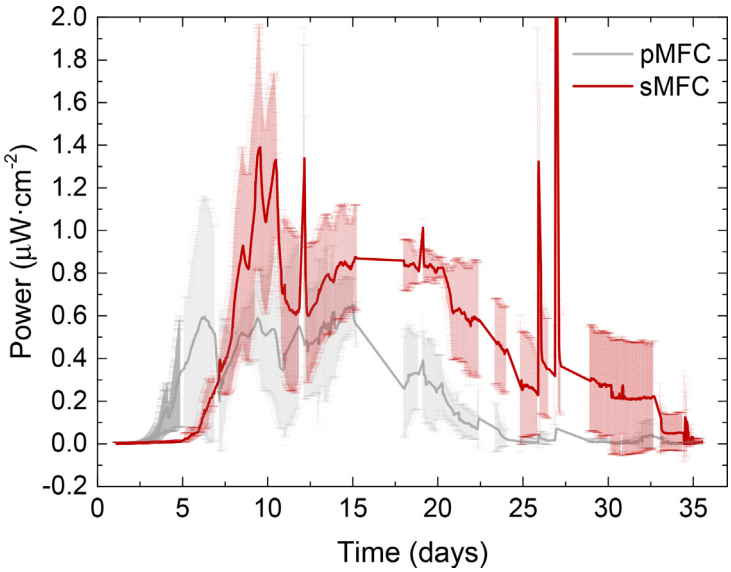

Fig. 3. Average and standard deviation of the power under operational conditions (1 kΩ) along the experiment in sMFCs (green line) and pMFCs (grey line). The data were measured in triple parallel tests.

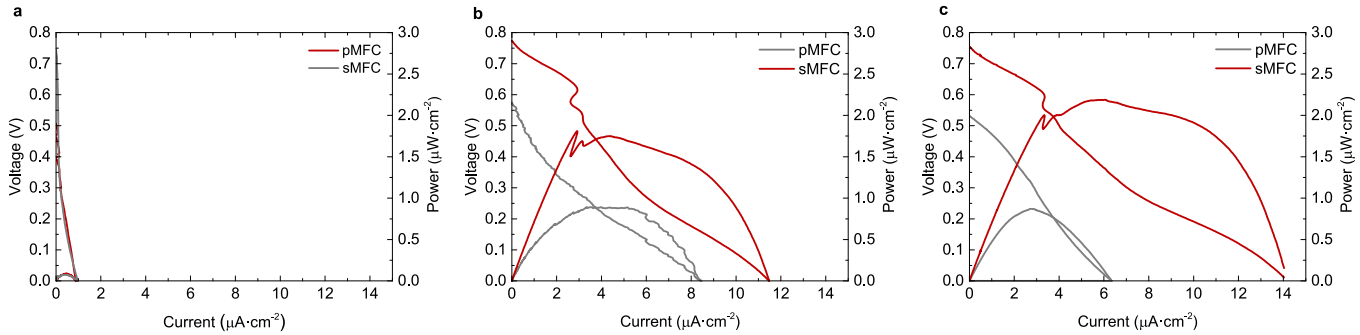

Fig. 4. I-V characteristic curves and power curves taken after 1 (a), 2 (b) and 3 weeks (c) of operation in one of the sMFC and pMFC reactors.

current production was observed throughout the experiment. In the case of sMFCs, the start-up period was longer, and voltage did not increase until d 5. However, sMFC reactors reached higher maximum power values of about 1.1 ± 0.2 μW·cm^{-2} at d 10, stabilizing at 0.84 ± 0.02 μW·cm^{-2} between d 15 and 20 of the study, indicating a best performance (Fig. 3). The cause of a faster start-up and, therefore, biofilm formation in the case of pMFC reactors may be associated to the presence of root exudates and root-derived organic compounds that, as already reported by Li et al. [20], may enhance the electrochemical reaction on the anode in the first days of operation, while the performance of sMFC depends on the use of different organic matters present in soil [21].

This trend was also observed in the I-V curves performed weekly. Fig. 4 shows representative I-V and power curves obtained with both types of MFC. Main parameters extracted from these curves are summarized in Table 1.

Table 1
Summary of the results extracted from the I-V and power curves for the two experimental setups (sMFC and pMFC) throughout the experiment. [1]Potential measured versus Ag/AgCl.

	pMFC				
Time (d)	**7**	**14**	**21**	**28**	**35**
OCP (mV)	674.67 ± 23.12	478.67 ± 159.95	398 ± 128.9	108.7 ± 60.12	107.33 ± 18.7
Imax (μA·cm^{-2})	3.37 ± 2.16	6.47 ± 2.9	5.9 ± 1.9	2.03 ± 1.7	0.9 ± 1.15
Pmax (μW·cm^{-2})	0.46 ± 0.33	0.65 ± 0.36	0.59 ± 0.31	0.06 ± 0.07	0.05 ± 0.08
OCPa (mV)[1]	−342 ± 86.61	−131 ± 93.72	−123.33 ± 166.81	258.33 ± 81.45	180 ± 137.36
OCPc (mV)[1]	332.67 ± 87.12	348 ± 66.46	274.7 ± 66.6	367 ± 27.18	287.3 ± 155.09
	sMFC				
Time (d)	**7**	**14**	**21**	**28**	**35**
OCP (mV)	715 ± 46.81	730 ± 55.02	735.67 ± 33.8	517.3 ± 33.8	478.4 ± 197.34
Imax (μA·cm^{-2})	0.82 ± 0.13	6.95 ± 3.91	11.27 ± 2.62	8.7 ± 1.9	8.1 ± 2.7
Pmax (μW·cm^{-2})	0.08 ± 0.02	1.52 ± 0.25	2 ± 0.22	1.2 ± 0.7	1.12 ± 0.5
OCPa (mV)[1]	−391.7 ± 2.08	−413.33 ± 9.02	−408 ± 7.21	−143.4 ± 225.02	−177.7 ± 150.6
OCPc (mV)[1]	323.4 ± 45.32	316.6 ± 63.52	327.66 ± 38.68	374 ± 72.55	300.6 ± 189.9

During the first week after the start-up period (Fig. 4a), both MFCs provided similarly high OCP values of 647 ± 23 (sMFC) and 715 ± 47 mV (pMFC). Additionally, the magnitude of the anode potential was also similar, with values of −392 ± 2 (sMFC) and −342 ± 86 mV (vs Ag/AgCl) (pMFC). This result indicated the existence of anaerobic conditions around the anodes in both reactors [22]. However, the capacity to sustain these high voltages over time differed between MFCs. pMFCs maintained higher voltages with the increment of the current, providing maximum power and current values 75% higher than sMFCs (Table 1). The maximum power values obtained by pMFCs are in consonance with other reference works such as Liu et al. [20] that obtained maximum power values of 0.7 ± 0.3 $\mu W \cdot cm^{-2}$ with a similar pMFC configuration. This result may be understood considering the higher substrate availability of pMFCs, something already reported and related to the presence of root exudates that reduced the internal resistance of the anode [23]. It should be noted that the high deviations observed in the case of pMFCs resulted from a slower start-up and growth of one of the replicates, which also considered in data analysis for completeness.

sMFC performance values increased greatly during the second week of operation (Fig. 4b). Maximum power and current magnitudes reached values of 6.95 $\mu A \cdot cm^{-2}$ and 1.52 $\mu W \cdot cm^{-2}$, respectively, which are very close to those obtained by pMFC reactors (6.47 $\mu A \cdot cm^{-2}$ and 0.46 $\mu W \cdot cm^{-2}$). Along the third week, the performance of the pMFCs significantly decreased, while the sMFCs reached their maximum with current and power values of 11.27 $\mu A \cdot cm^{-2}$ and 2 $\mu W \cdot cm^{-2}$ (Fig. 4c). After 28 d of operation, sMFC performance is reduced to 8.7 ± 1.9 $\mu A \cdot cm^{-2}$, in the same order that current values obtained in other works. For example, Donovan et al. [12] obtained current maximum values of 4 $\mu A \cdot cm^{-2}$ after 30 d of operation.

Although the maximum power value obtained during the experiment was very different, 1.99 ± 0.22 $\mu W \cdot cm^{-2}$ and 0.6 ± 0.4 $\mu W \cdot cm^{-2}$ for sMFC and pMFC, respectively (Fig. 5a), both devices produced a similar amount of electrical energy (Fig. 5b) by the higher internal resistance of the pMFCs.

The variation in the cathode and anode potentials along the experiment is also presented in Table 1. No significant changes were observed in cathode potentials along the study in both MFCs, while the anode potential experienced an important variation during operation. This change in the anode potential was more pronounced in the case of pMFCs, which varied from the initial −342 ± 86.61 mV towards positive values at the end of the experiment, i.e. 287.3 ± 155.09 mV. sMFCs, on the other hand, maintained negative potentials in the anode for the duration of the experiment, from −391.7 ± 2.08 to −177.7 ± 150.6 mV. This high variation of the anode potential resulted in lower electric voltages and performance of the pMFCs and may be attributed to the presence of oxygen in the anode proximity. Oxygen in the anode of the MFC has been already demonstrated to increase the anode potential due to chemical oxygen reduction, leading to higher anode resistances [22]. The origin of the oxygen may be plant-roots, which already reported to release oxygen into the rhizosphere in submerged conditions [24]. In the case of the self-contained pMFCs developed in this work, plant-roots were clearly growing through the anode felt (Fig. 6), which likely resulted in local variations of exudation and radial oxygen loss and thus, in the availability of electron donors and acceptor [22]. These results are in line with different studies analysing the influence of the distance between roots and anode electrode [20,25], which concluded that there is no optimal option to place the anode in the proximity of the rhizosphere for high-power generation but it should be placed far from it. This solution was not possible in a closed, portable and self-containing pMFC with limited space such as the developed in this work. Although initially the anode electrode was positioned in a separation of 3 cm from the plant, roots surrounded completely the 3 cm of substrate by the end of the experiment, being in direct physical contact with the electrode.

sMFC voltage started to decrease after 20 d of operation, which associated with organic matter depletion [7] since substrate concentration plays a very significant role in the operation and performance of MFC [26]. pMFCs were here advantageous since the living plant ensured a continuously delivery of substrate in the proximity of the anode and thus an uninterrupted and sustained power production [6].

3.4. Combination of soil and plant MFCs in self-contained hybrid architectures

Although considerable enhancements have been made, the continuous supply of organic matter to improve electricity generation of sMFCs is still a challenge to sustain long-term operations. This could be solved in pMFCs although the problems associated with the diffusion of oxygen from the roots, and the impossibility in a closed and portable system to increase the roots-electrode distance do not allow to improve the performance in applications such as portable energy sources. As an alternative, hybrid sMFC/pMFCs self-containing structures were developed as a proof-of-concept (Fig. 7a), where two independent compartments are assembled in a single MFC: one containing the plant and another with a fully operational sMFC. Plant and sMFC were connected in such a way that the plant leachate, produced after irrigation, was led to the sMFC. In this way, we obtained the advantages of both

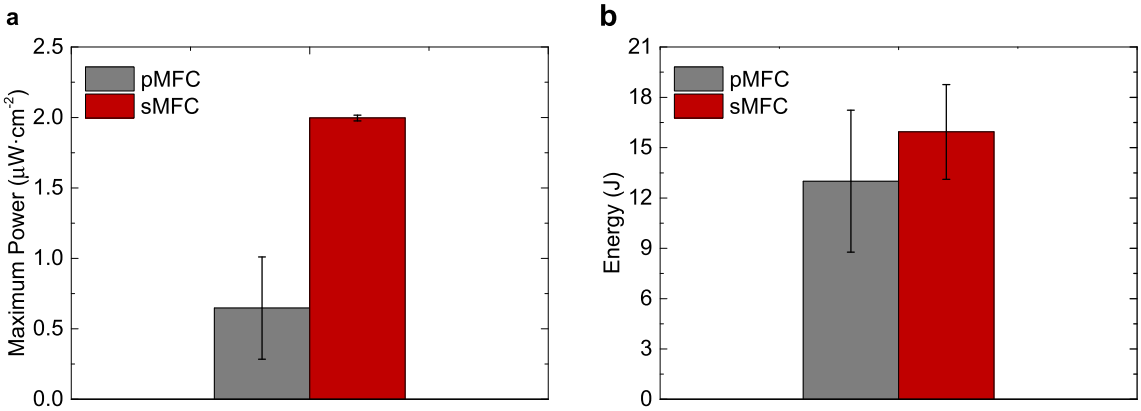

Fig. 5. Maximum power values (a) and total energy (b) produced during the experiment in sMFC and pMFC reactors.

Fig. 6. Images of the roots and anode electrode of a dismantled pMFC at the end of the experiment and cross section of plant root. Aerenchyma is indicated with a red mark.

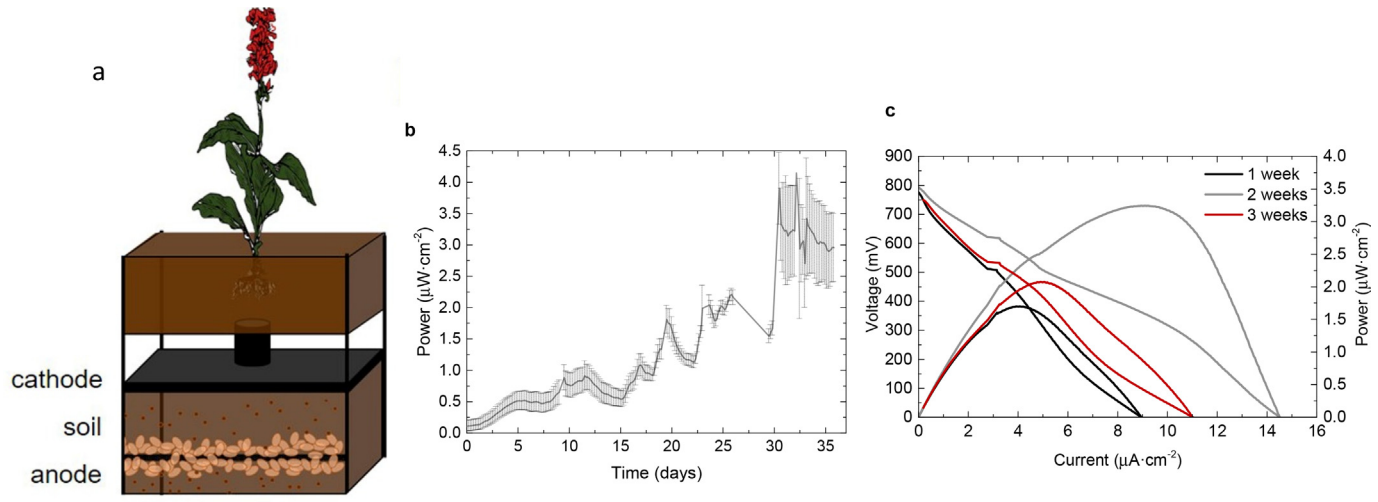

Fig. 7. (a). Schematic representation of the hybrid-MFC. (b). Average and standard deviation of the power obtained by three hybrid-MFC running in parallel for one month. (c). I-V characteristic curves and power curves taken after 1, 2 and 3 weeks of operation in one of the hybrid-MFCs.

technologies (sMFC and pMFC), i.e. long term stability thanks to continuous nutrient supply from the plant leachate to microorganisms in the anode, while ensure high performance by minimizing the transport of oxygen from the plant-roots to the anode, which allocated far from the plant in a separated compartment. The average of the power obtained by three hybrid-MFC devices along 1 month is presented in Fig. 7b.

Thus, after two weeks of slow growth, power vales increased considerably until reaching the maximum of 3.5 ± 0.57 $\mu W \cdot cm^{-2}$ at d 30. Drops in power observed at d 20 and 26 of operation were caused by an obstruction of the leachate conduit between the two containers. The clear trend to power increase can also be observed in the power curves performed at different times during the operation of the hybrid-MFCs (Fig. 7c). Thus, maximum current and power values increased along time reaching values of 14.51 $\mu A \cdot cm^{-2}$ and 3.24 $\mu W \cdot cm^{-2}$ after 3 weeks of operation.

The total energy generated by these devices during a month was 1583.67 ± 157.75 J. In order to compare this energy to that obtained by the sMFC and pMFC devices used previously, energy was calculated from the power data normalized by the area of the electrodes. This resulted in a total energy of 0.14 ± 0.044 and 0.17 ± 0.03 J per cm^2 of electrode for the pMFC and sMFC respectively, while the hybrid-MFC produced 1.8 ± 0.17 J per cm^2 of electrode indicating its best performance.

Although still requiring intensive studies and evaluations, these new hybrid technologies and designs may overcome the problems of these systems for real life applications.

4. Conclusions

Self-containing MFCs minimize the drawbacks of current MFCs when operating in field and speed up the transference of these technologies from the laboratory to the real environments. From the two self-containing configurations developed, sMFCs presented better performances in general, with higher continuous power generated (maximum of 0.46 ± 0.21 $\mu W \cdot cm^{-2}$). The lower performance of pMFCs is associated to the negative effects of

root-plants on anode potential releasing oxygen that increases the anode resistance. On the other hand, pMFCs presented shorter start-up times (3 d), which associated with the continuous nutrients supply from the plant to the bacteria in the anode. An initial proof-of-concept of a self-containing sMFC/pMFC technology shows promising results for in field applications, such as long-term power supply of low-power field electronic devices, from meteorological sensors or LED lights, although extensive evaluation is still necessary to confirm these initial results.

Financial support

This work was supported by the European Union's Horizon 2020 SME instruments programme under grant agreement No 767678 and "GrowBot" European Project (FET Proactive: emerging paradigms and communities, Research and Innovation Action Grant agreement n. 824074). X.M.B. acknowledges financial support from the Spanish Ministry of Economy and Competitiveness (SMARTECOPONICS project PCIN-2017-031). N.U is supported by Torres Quevedo Programme Grant Number PTQ2019-010641 / AEI / https://doi.org/10.13039/501100011033. N.U, R-D.C, C.N and L.K acknowledge support from Pablo Vidarte and Arkyne technologies S.L. (BIOO).

Conflict of interest

The authors declare that they have no known competing financial interests or personal relationships that could have appeared to influence the work reported in this paper.

Supplementary data

https://doi.org/10.1016/j.ejbt.2022.04.004.

References

[1] Regmi R, Nitisoravut R, Ketchaimongkol J. A decade of plant-assisted microbial fuel cells: Looking back and moving forward. Biofuels 2018;9(5):605–12. https://doi.org/10.1080/17597269.2018.1432272.

[2] Abbas SZ, Rafatullah M, Ismail N, et al. A review on sediment microbial fuel cells as a new source of sustainable energy and heavy metal remediation: Mechanisms and future prospective. Int J Energy Res 2017;41(9):1242–64. https://doi.org/10.1002/er.3706.

[3] Zabihallahpoor A, Rahimnejad M, Talebnia F. Sediment microbial fuel cells as a new source of renewable and sustainable energy: Present status and future prospects. RSC Adv 2015;5(114):94171–83. https://doi.org/10.1039/C5RA15279H.

[4] Prasad J, Tripathi RK. Energy harvesting from sediment microbial fuel cell to supply uninterruptible regulated power for small devices. Int J Energy Res 2019;43(7):2821–31. https://doi.org/10.1002/er.4370.

[5] Abbas SZ, Rafatullah M. Recent advances in soil microbial fuel cells for soil contaminants remediation. Chemosphere 2021;272:. https://doi.org/10.1016/j.chemosphere.2021.129691 PMid: 33573807129691.

[6] Strik DP, Hamelers HVM, Snel JFH, et al. Green electricity production with living plants and bacteria in a fuel cell. Int J Energy Res 2008;32(9):870–6. https://doi.org/10.1002/er.1397.

[7] Chicas SD, Sivasankar V, Omine K, et al. Plant microbial fuel cell technology: developments and limitations. In: Sivasankar V, Mylsamy P, Omine K (eds). Microbial Fuel Cell Technology for Bioelectricity. Springer, Cham. 2018:49–65. 10.1007/978-3-319-92904-0_3.

[8] Rossi M, Tosato P, Gemma L, et al. Long range wireless sensing powered by plant-microbial fuel cell. Design, Automation & Test in Europe Conference & Exhibition. 2017:1651–1654. 10.23919/DATE.2017.7927258.

[9] Strik DP, Timmers RA, Helder M, et al. Microbial solar cells: Applying photosynthetic and electrochemically active organisms. Trends Biotechnol 2011;29(1):41–9. https://doi.org/10.1016/j.tibtech.2010.10.001 PMid: 21067833.

[10] Helder M, Strik DP, Hamelers HVM, et al. The flat-plate plant-microbial fuel cell: The effect of a new design on internal resistances. Biotechnol Biofuels 2012;5:70. https://doi.org/10.1186/1754-6834-5-70 PMid: 22998846.

[11] Brunelli D, Tosato P, Rossi M. Flora health wireless monitoring with plant-microbial fuel cell. Procedia Eng 2016;168:1646–50. https://doi.org/10.1016/j.proeng.2016.11.481.

[12] Donovan C, Dewan A, Heo D, et al. Batteryless, wireless sensor powered by a sediment microbial fuel cell. Environ Sci Technol 2008;42(22):8591–6. https://doi.org/10.1021/es801763g PMid: 19068853.

[13] Chen S, He G, Liu Q, et al. Layered corrugated electrode macrostructures boost microbial bioelectrocatalysis. Energy Environ Sci 2012;5(12):9769–72. https://doi.org/10.1039/c2ee23344d.

[14] Gregory KB, Lovley DR. Remediation and recovery of uranium from contaminated subsurface environments with electrodes. Environ Sci Technol 2005;39(22):8943–7. https://doi.org/10.1021/es050457e PMid: 16323798.

[15] Goto Y, Yoshida N, Umeyama Y, et al. Enhancement of electricity production by graphene oxide in soil microbial fuel cells and plant microbial fuel cells. Front Bioeng Biotechnol 2015;3:42. https://doi.org/10.3389/fbioe.2015.00042 PMid: 25883931.

[16] Wang H, Park J-D, Ren ZJ. Practical energy harvesting for microbial fuel cells: A review. Environ Sci Technol 2015;49(6):3267–77. https://doi.org/10.1021/es5047765 PMid: 25670167.

[17] Nguyen N, Nguyen D, Taguchi K. A novel design portable plugged-type soil microbial fuel cell for bioelectricity generation. Energies 2021;14(3):553. https://doi.org/10.3390/en14030553.

[18] Helder M, Strik DP, Hamelers HVM, et al. New plant-growth medium for increased power output of the plant-microbial fuel cell. Bioresour Technol 2012;104:417–23. https://doi.org/10.1016/j.biortech.2011.11.005 PMid: 22133604.

[19] Timmers RA, Strik DP, Hamelers HVM, et al. Long-term performance of a plant microbial fuel cell with Spartina anglica. Appl Microbiol Biotechnol 2010;86:973–81. https://doi.org/10.1007/s00253-010-2440-7 PMid: 20127236.

[20] Liu B, Ji M, Zhai H. Anodic potentials, electricity generation and bacterial community as affected by plant roots in sediment microbial fuel cell: Effects of anode locations. Chemosphere 2018;209:739–47. https://doi.org/10.1016/j.chemosphere.2018.06.122 PMid: 29960941.

[21] Umar MF, Abbas SZ, Ibrahim MNM, et al. Insights into advancements and electrons transfer mechanisms of electrogens in benthic microbial fuel cells. Membranes 2020;10(9):205. https://doi.org/10.3390/membranes10090205 PMid: 32872260.

[22] Timmers RA, Strik DP, Arampatzoglou C, et al. Rhizosphere anode model explains high oxygen levels during operation of a *Glyceria maxima* PMFC. Bioresour Technol 2012;108:60–7. https://doi.org/10.1016/j.biortech.2011.10.088 PMid: 22265596.

[23] Wetser K, Dieleman K, Buisman C, et al. Electricity from wetlands: Tubular plant microbial fuels with silicone gas-diffusion biocathodes. Appl. Energy. 2017;185(Part 1):642–649. 10.1016/j.apenergy.2016.10.122.

[24] Jackson MB, Armstrong W. Formation of aerenchyma and the processes of plant ventilation in relation to soil flooding and submergence. Plant Biol 1999;1(3):274–87. https://doi.org/10.1111/j.1438-8677.1999.tb00253.x.

[25] Xu F, Cao F, Kong Q, et al. Electricity production and evolution of microbial community in the constructed wetland-microbial fuel cell. Chem Eng J 2018;339:479–86. https://doi.org/10.1016/j.cej.2018.02.003.

[26] Nawaz A, Hafeez A, Abb SZ, et al. A state of the art review on electron transfer mechanisms, characteristics, applications and recent advancements in microbial fuel cells technology. Green Chem Lett Rev 2020;13(4):365–81. https://doi.org/10.1080/17518253.2020.1854871.